First report of *Ovipleistophora ovariae* and *O. diplostomuri* in China provides new insights into the intraspecific genetic variation and extends their distribution

Meiqi Weng[1,2,3] (iD), Derong Xie[1,2,3], Qianqian Zhang[2], Aihua Li[2]
and Jinyong Zhang[1] (iD)

[1]The Laboratory of Aquatic Parasitology, School of Marine Science and Engineering, Qingdao Agricultural University, 266237 Qingdao, China; [2]Key Laboratory of Aquaculture Diseases Control, Ministry of Agriculture and State Key Laboratory of Freshwater Ecology and Biotechnology, Institute of Hydrobiology, Chinese Academy of Sciences, Wuhan 430072, China and [3]College of Advanced Agricultural Sciences, University of Chinese Academy of Sciences, Beijing 10049, China

Abstract

Microsporidia of the genus *Ovipleistophora* are generally parasites of fishes and aquatic crustaceans. In the current study, *Ovipleistophora diplostomuri* and *O. ovariae* were firstly reported from *Culter alburnus* and *Xenocypris argentea* and *Parabramis pekinensis*, respectively. Both of them exclusively infected fish ovary and were morphologically, ultrastructurally and genetically characterized. Sporogony occurred in direct contact with the host cell cytoplasm and sporophorous vesicles were not observed for the new isolates of these two *Ovipleistophora* species. Spores of *O. ovariae* were for the first time observed to be dimorphic. Genetic analysis indicated that the genetic variation in the ITS and LSU sequences was distinct among between-host *O. diplostomuri* isolates. High sequence variation in ITS sequence suggests that it can be a reliable molecular marker to explore the population genetics of *O. diplostomuri*. This is the first report of these two *Ovipleistophora* species in China which extends their host and geographical range.

Introduction

Microsporidia are obligate intracellular eukaryotic parasites that infect most animal taxa (Stentiford *et al.*, 2013; Cali and Takvorian, 2014). More than 1500 microsporidia belonging to about 220 genera have been reported worldwide, among which around half genera are known to infect aquatic organisms, including fish, aquatic arthropods and aquatic non-arthropod invertebrates, as well as protists (Stentiford *et al.*, 2013; Vávra *et al.*, 2017; Park and Poulin, 2021). Fish are the common hosts of aquatic microsporidia and some fish-infecting microsporidia are known to cause disastrous diseases in aquaculture (Vávra and Lukeš, 2013; Kent *et al.*, 2014). More than 160 species belonging to about 22 genera are known to infect fishes (Liu *et al.*, 2019). Although a few fish-infecting microsporidia have a broad host range, the majority of species show a comparative strict host specificity (Summerfelt and Goodwin, 2010; Kent *et al.*, 2014). Recent evidence showed that phylogenetic relationships between microsporidia were linked to their host and the infected tissues (Smith, 2009; Stentiford *et al.*, 2013; Vávra and Lukeš, 2013). Therefore, host and tissue information are thought to be important for the classification of Microsporidia.

Based on the morphological and molecular difference of *Pleistophora mirandellae* and *P. ovariae* from the fish trunk muscle-infecting *Pleistophora* species, Pekkarinen *et al.* (2002) erected a genus *Ovipleistophora* to accommodate these two microsporidia and defined that the genus *Ovipleistophora* had a tissue tropism for ovary of fish. However, the recently reported two *Ovipleistophora* species did not follow the definition. Among them, *O. diplostomuri* infects the liver of the bluegill sunfish *Lepomis macrochirus* and the metacercarial cyst wall of the digenean parasite *Posthodiplostomum minimum* (Lovy and Friend, 2017). *O. arlo* infects the musculature of the common prawn *Palaemon serratus* (Stentiford *et al.*, 2018). Moreover, Bojko *et al.* (2020) found that *O. diplostomuri* can also infect the musculature of the crayfish *Procambarus bivittatus*. Therefore, based on the above findings it was proposed that *Ovipleistophora* species have a broad host range or utilize crustaceans in a multi-host life-cycle. Further elucidating the tissue tropism, host specificity and geographical distribution of the genus *Ovipleistophora* will undoubtedly deepen insights into the classification and evolutionary biology of this group of microparasites. As a part of an ongoing project to investigate the diversity of aquatic microsporidia in the middle and lower reaches of the Yangtze River, two fish-infecting microsporidia from the ovary of three different fishes were for the first time reported. Morphological and molecular characterization indicated that these two species are affiliated to the genus *Ovipleistophora* and this finding extends their host and geographical range. Remarkable intraspecific genetic variation referred from ITS and LSU molecular marker were distinct for between-host *Ovipleistophora diplostomuri* isolates.

CAMBRIDGE
UNIVERSITY PRESS

Materials and methods

Sample collections

Culter alburnus and *Xenocypris argentea* were captured by gill nets from the Danjiangkou Reservoir located between the northwest of Hubei province and the southwest of Henan province, China (32°55′ 38.46″N, 111° 34′ 27.44″E) in April 2019. *Parabramis pekinensis* was captured by gill nets from the Yangtze Estuary, China (31°34′ 44.17″N, 121°37′50.89″E) in August 2019. Specimens were held on ice and transported immediately to the local laboratory for the preliminary parasitological examination. Fish were anaesthetized by an overdose of MS 222 (Sigma, Germany) and then subjected for necropsy. Microsporidian infections were screened by the presence of visible whitish cysts embedded in ovaries. The cysts were ruptured to prepare wet mounts which were observed at 1000× with an oil immersion objective to determine the microsporidian infection. The microsporidian cysts and cysts-containing tissue samples were preserved in 95% ethanol for further molecular characterization and in 2.5% glutaraldehyde in 0.1 M sodium cacodylate buffer (PH 7.4) for electron microscopic observation, as well as in 10% neutral buffered formalin for morphological and histological analysis, respectively. Formalin-fixed spores were used to capture spore images using an Olympus BX 53 microscope equipped with an Olympus DP72 digital camera (Olympus, Japan).

Histological examination

Cyst-containing tissue samples from the ovaries of the infected fish fixed in 10% neutral-buffered formalin were dehydrated through a series of graded concentrations of ethanol and embedded in paraffin wax. Tissue sections, 3 μm in width, were stained with haematoxylin and eosin (H&E) and examined under a light microscope (Olympus, Japan) (Liu *et al.*, 2018).

Transmission electron microscopy (TEM) observation

Glutaraldehyde-fixed cysts were washed three times for 10 min in sodium cacodylate buffer and then fixed with 1% osmium tetroxide (OsO4) in the same buffer for 1 h. After dehydration through a gradually ascending series of ethanol and propylene oxide, samples were embedded in Spur resin. Ultrathin sections (70–90 nm) were mounted on an uncoated copper grid and stained with uranyl acetate and lead citrate (Liu *et al.*, 2019). Sections of two cysts were examined using a Hitachi HT-7700 transmission electron microscope (TEM).

DNA extraction, polymerase chain reaction (PCR), and sequencing

Ethanol-fixed cysts were washed with distilled water three times to remove ethanol remnants. The genomic DNA was extracted using the Qiagen DNeasy Blood & Tissue Kit (Qiagen, Germany) with the assistance of a Fast Prep cell disruptor 1 min at 6 m s^{-1} (MP Biomedicals, USA) following the manufacturer's instructions. The primer sets used for rRNA gene amplification are shown in Table 1. PCR was carried out in a 50 μL reaction system, containing PCR buffer, 200 mM dNTP, 2 mM MgCl$_2$, 1.25 units Taq polymerase, 20 pmol each primer, and 2 μL DNA template. The partial SSU rDNA was amplified using the primer pair V1f/1492r and the PCR cycle consisted of an initial denaturation step at 95°C for 4 min, followed by 35 cycles at 95°C for 1 min, 50°C for 30 s, 72°C for 2 min, and a final extension at 72°C for 10 min. For some taxa, for which the primer pair V1f/1492r did not work the primer pair V1f/1047r was applied, with thermocycler parameters as follows: an initial denaturation step at 94°C for

Table 1. The primers used for amplifying and sequencing microsporidia rDNA

Primer	Sequence (5′-3′)	References
V1F	CACCAGGTTGATTCTGCCTGAC	Weiss and Vossbrinck (1999)
1047r	AACGGCCATGCACCAC	Baker *et al.* (1995)
1492r	GGTTACCTTGTTACGACTT	Weiss and Vossbrinck (1999)
HG4F	GCGGCTTAATTTGACTCAAC	Gatehouse and Malone (1998)
ILSUR	ACCTGTCTCACGACGGTCTAAAC	Tsai *et al.* (2002)

4 min, followed by 35 cycles at 94°C for 30 s, 48°C for 30 s, 72°C for 1 min and a final extension at 72°C for 10 min. The 3′ terminal partial SSU rDNA, complete ITS and the partial LSU rDNA sequence was amplified using the primer pair HG4F/ILSUR and the PCR cycle consisted of an initial denaturation step at 95°C for 4 min, followed by 35 cycles at 95°C for 30 s, 53°C for 30 s, 72°C for 2 min, and a final extension at 72°C for 10 min. The PCR products were excised from an agarose gel and purified using a PCR purification kit (CWBiotech, Beijing, China) and cloned into the PMD-18 T vector system (Takara, Tokyo, Japan). Then positive clones were randomly selected for sequencing in both directions with the ABI BigDye Terminator v3.1 Cycle Sequencing Kit and an ABI 3100 Genetic Analyzer.

Phylogenetic analysis

The obtained all sequences of fragments were assembled by BioEdit (Hall, 1999) to produce consensus sequences which were applied to determine their matching species by a BLAST search. Sequences with high similarity and those of interest were retrieved from the GenBank database. A total of 23 sequences were aligned with Clustal X by the default setting (Thompson *et al.*, 1997). This alignment was corrected manually using the alignment editor function within MEGA 6.0 (Tamura *et al.*, 2013). *Dictyocoela berillonum* (KM657354) was used as an outgroup. Pairwise genetic distances/similarities were calculated using the Kimura-2 parameter model distance matrix for transitions and transversions. Phylogenetic analyses were conducted using the maximum likelihood (ML) method in PhyML 3.0 and Bayesian inference (BI) in MrBayes 3.2.4, respectively. The optimal evolutionary model was determined to be GTR + I + G by ModelTest 3.7 using the Akaike information criteria. Two independent runs were conducted with four chains for one million generations for BI. Phylogenetic trees were sampled every 100 generations. The first 25% of the samples were discarded from the cold chain (burninfrac = 0.25). Bootstrap confidence values were calculated with 100 repetitions for ML. The tree was initially examined in Figtree v1.4.4 (http://tree.bio.ed.ac.uk/software/figtree/), edited and annotated in Adobe Illustrator (Adobe System, San Jose, CA, USA).

Results

Macroscopical and light microscopical observations

All sampled fish did not appear any external disease symptoms. After necropsy, macroscopic whitish cysts embedded in the ovary of one out of 14 (prevalence: 7.1%) *C. alburnus* (Fig. 1a), 1 out of 6 (prevalence: 16.7%) *X. argentea* (Fig. 1b) sampled from the Danjiangkou Reservoir and 1 of 2 (prevalence: 50%) *P. pekinensis* (Fig. 1c) sampled from the Yangtze Estuary. The cysts from *C. alburnus* were oval and whitish-opaque in
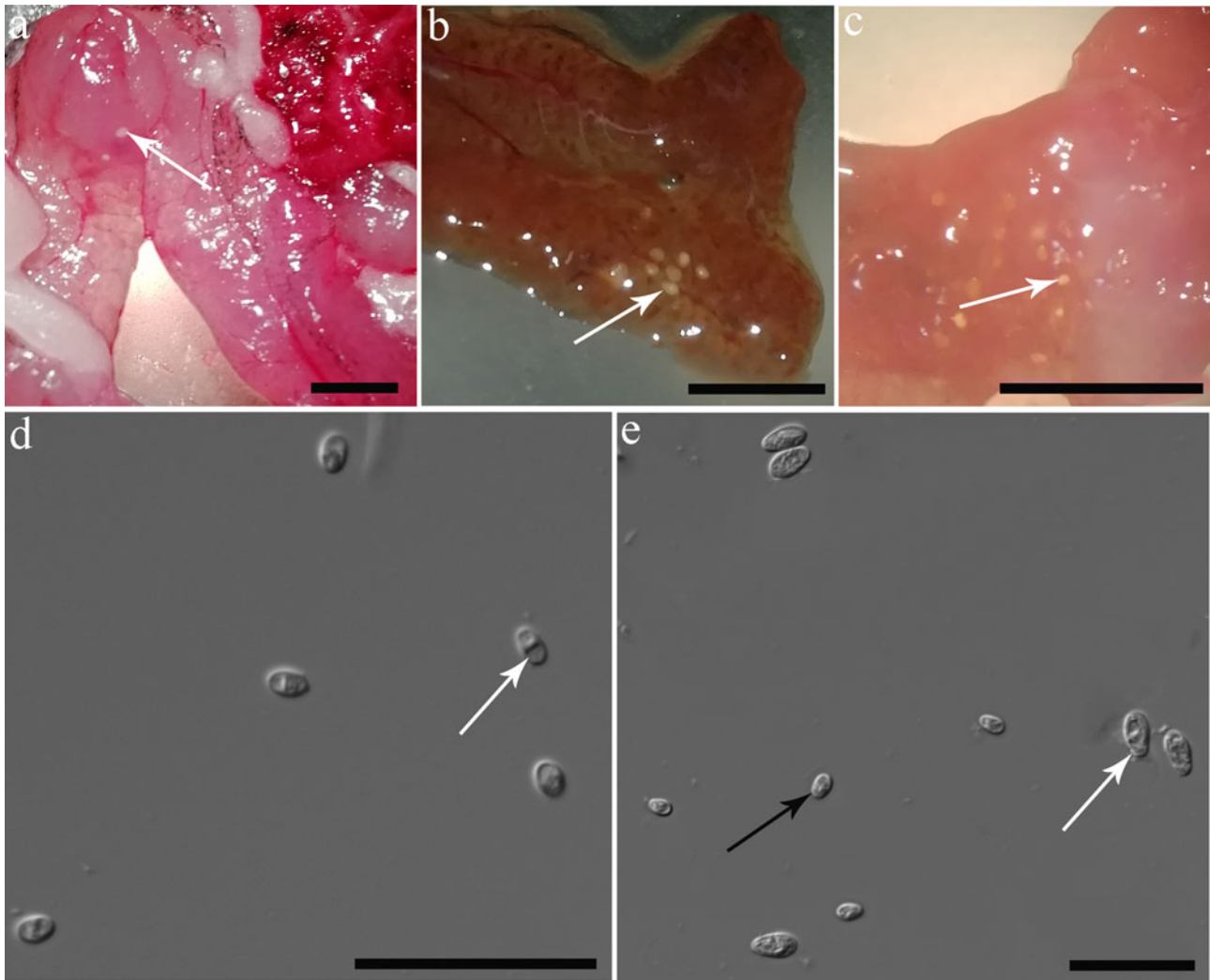
Fig. 1. Macroscopical observation and light microscopy of *Ovipleistophora* species isolated from the ovary of different fishes. (a) Cyst (arrow) isolated from the ovary of *Culter alburnus* was macroscopically visible. Scale bar = 5 mm. (b) Cyst (arrow) isolated from the ovary of *Xenocypris argentea* was macroscopically visible. Scale bar = 5 mm. (c) Cyst (arrow) isolated from the ovary of *Parabramis pekinensis* was macroscopically visible. Scale bar = 5 mm. (d) Fresh spores of *O. diplostomuri* isolated from the *Culter alburnus* observed under light microscopy, the posterior vacuole (arrow) distinctly located at the posterior end of spores. Scale bar = 20 μm. (e) Macrospores (white arrow) and microspores (black arrow) of *O. ovariae* isolated from the *P. pekinensis* were observed under light microscopy. Scale bar = 20 μm.

colouration, measuring 612.3 (498.1–791.8) μm long and 419.6 (318.7–567.7) μm wide ($N = 15$) (Fig. 1a). Monomorphic spores enclosed within the cysts were oval (Fig. 1d), measuring 4.03 ± 0.23 (3.74–4.54) μm long and 2.63 ± 0.17 (2.40–2.94) μm wide ($N = 40$). Cysts from *X. argentea* were slightly larger than those from *C. alburnus*, which were pyriform and whitish-opaque in colouration, measuring 761.2 (691.1–815.1) μm long and 434.5 (371.78–490.9) μm wide ($N = 15$) (Fig. 1b). Monomorphic spores enclosed within the cysts from *X. argentea* were also oval and measured 4.03 ± 0.3 (3.43–4.60) μm long and 1.94 ± 0.14 (1.60–2.20) μm wide ($N = 40$). Cysts from *P. pekinensis* were of irregular shape (Fig. 1c) where were filled with a mass of dimorphic spores, both of which were oval. Microspores measured 4.17 ± 0.29 (3.70–4.67) μm long and 2.72 ± 0.21 (2.30–3.20) μm wide ($N = 40$) and macrospores measured 9.26 ± 0.36 (8.61–10.13) μm long and 4.90 ± 0.15(4.59–5.19) μm wide ($N = 40$) (Fig. 1e).

Histological examination

Histopathological observations showed that the cysts from the three fish hosts developed the connective tissue of ovary parenchyma between oocytes (Fig. 2). The wall of cysts from *C. alburnus* and *X. argentea* were significantly thicker than that of cysts

from *P. perkinensis* (Fig. 2b, d and f). The somatic cells in the ovary were distinctly attached the connective tissue layer of the cyst wall (Fig. 2b and f). No remarkable inflammatory responses were observed in the infected ovaries.

TEM

Sporoblasts and mature spores were observed for both microsporidian species from both *C. alburnus* and *P. pekinensis* and only mature spores could be found for species from *X. argentea* under electron microscopy. Sporoblasts isolated from the ovary of *C. alburnus* were of irregular shape and electron-dense which were surrounded by a thick electron-dense membrane (Fig. 3a). Only monomorphic mature spores were found which were uninucleate. Mature spores were in direct contact with the host cell cytoplasm (Fig. 3g). A large posterior vacuole occupying the half volume of spores was visible in the posterior end of spores (Fig. 3b). Isofilar polar filaments coiled 8–10 coils and arranged in one row (Fig. 3b). The polar filament measured 112–122 nm in diameter and could be stratified with six discontinuous density concentric circles which included from outside to inside a 3 nm thick unit membrane, a 4 nm thick moderately electron-lucent layer, a 2 nm thick electron-dense layer, a 12 nm thick moderately
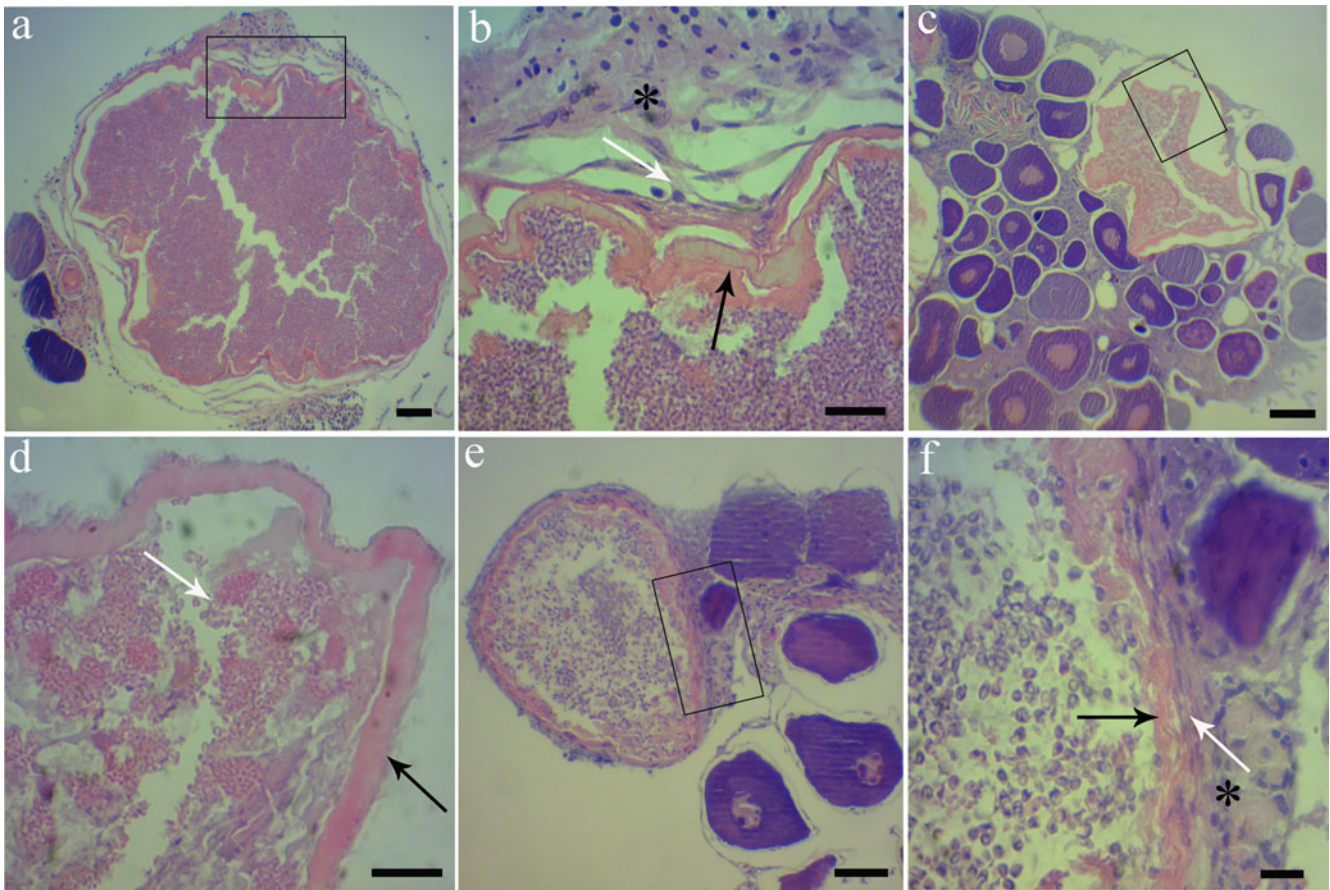
Fig. 2. Histopathology of the ovary of 3 fish species with infection of *Ovipleistophora* spp. (a) Large parasite-filled cysts isolated from the ovary of *Culter alburnus* were surrounded by connective tissue. Scale bar = 50 μm. (b) Higher magnification of the boxed area in Fig. 2a showing the thickened cyst wall (black arrow) surrounded with a layer of connective tissue (white arrow) where was attached with massive somatic cells (*) were visible. Scale bar = 20 μm. (c) Large parasite-filled cysts isolated from the ovary of *Xenocypris argentea* developed in the connective tissue between the oocytes. Scale bar = 200 μm. (d) Higher magnification of the boxed area in Fig. 2c shows large amounts of microsporidian spores (white arrow) within the cyst and the thickened cyst wall (black arrow). Scale bar = 20 μm. (e) Parasite-filled cyst isolated from the ovary of *Parabramis pekinensis* was surrounded by a layer of connective tissue. Scale bar = 50 μm. (f) Higher magnification of the boxed area in Fig. 2e shows the cyst wall (black arrow) and a thin surrounding connective tissue layer (white arrow) where were attached with massive somatic cells (*). Scale bar = 20 μm.

dense layer, a 10 nm thick moderately electron-lucent layer and a wide lucent centre (Fig. 3c). The spore wall was trilaminar, including a 43–46 nm thick electron-dense exospore, a 61–68 nm thick electron-lucent endospore and a 4–8 nm thick plasma membrane. The exospore consisted of two layers, including an electron-dense layer (layer 1) and a moderately electron-dense layer (layer 2) (Fig. 3c). The polaroplast was bipartite with a narrow anterior lamella and a wide posterior lamella (Fig. 3d). An umbrella-shaped anchoring disc located in the apex of spores was surrounded by the polaroplast (Fig. 3d). Mature spores isolated from *X. argentea* ultrastructurally resemble with those from *C. alburnus*. Monomorphic spores were uninucleate. Isofilar polar filaments coiled 8–10 coils and arranged in one row (Fig. 3e). The spore wall consisted of a 56–60 nm thick electron-dense exospore, a 39–44 nm thick electron-lucent endospore and a 3–5 nm thick plasma membrane. The exospore constituted of two layers, including an electron-dense layer (layer 1) and a moderately electron-dense layer (layer 2) (Fig. 3f). Sporoblasts isolated from the ovary of *P. pekinensis* were also of irregular shape and surrounded by a trilaminar electron-dense membrane (Fig. 4a). The transition of uninucleate sporoblasts to mature spores involved the differentiation of typical spore structures, including the anchoring disk, trilaminar spore wall, polar filaments and polaroplast. Mature spores were dimorphic. The structures of macrospores and microspores are similar, including a bipartite polaroplast with anterior lamellae and

posterior tubules, a large posterior vacuole, an umbrella-shaped anchoring disc located at the apex of spore and three layers of spore wall (Figs 4b–d and 5a–d). Mature spores were in direct contact with the host cell cytoplasm (Fig. 4e). The exospore of microspores and macrospores consisted of two layers, including an electron-dense layer (layer 1) and a moderately electron-dense layer (layer 2) (Figs 4c and 5c). Isofilar polar filaments of microspores coiled 6–10 coils and arranged in one row (Fig. 4b and c). The spore wall of microspores consisted of a 53–58 nm thick electron-dense exospore, a 46–52 nm thick electron-lucent endospore and a 6–8 nm thick plasma membrane (Fig. 4c). Isofilar polar filaments of macrospores coiled 19–34 coils and arranged in one to three rows (Fig. 5a and b). The polar filament of macrospores measured 162–178 nm in diameter and exhibited seven discontinuous density concentric circles which included from outside to inside a 4 nm thick unit membrane, a 4 nm thick moderately electron-lucent layer, a 3 nm thick electron-dense layer, a 9 nm thick moderately electron-lucent layer, a 10 nm thick moderately electron-dense layer, a 10 nm thick moderately electron-lucent layer and a wide lucent centre (Fig. 5c). The spore wall of the macrospore constituted of a 23–51 nm thick electron-dense exospore, a 53–96 nm thick electron-lucent endospore and a 5–8 nm thick plasma membrane (Fig. 5c). Given the similar ultrastructural features and typical infection site (ovary), these 3 species herein can be assigned to the genus *Ovipleistophora* (Microsporidia: Pleistophoridae).
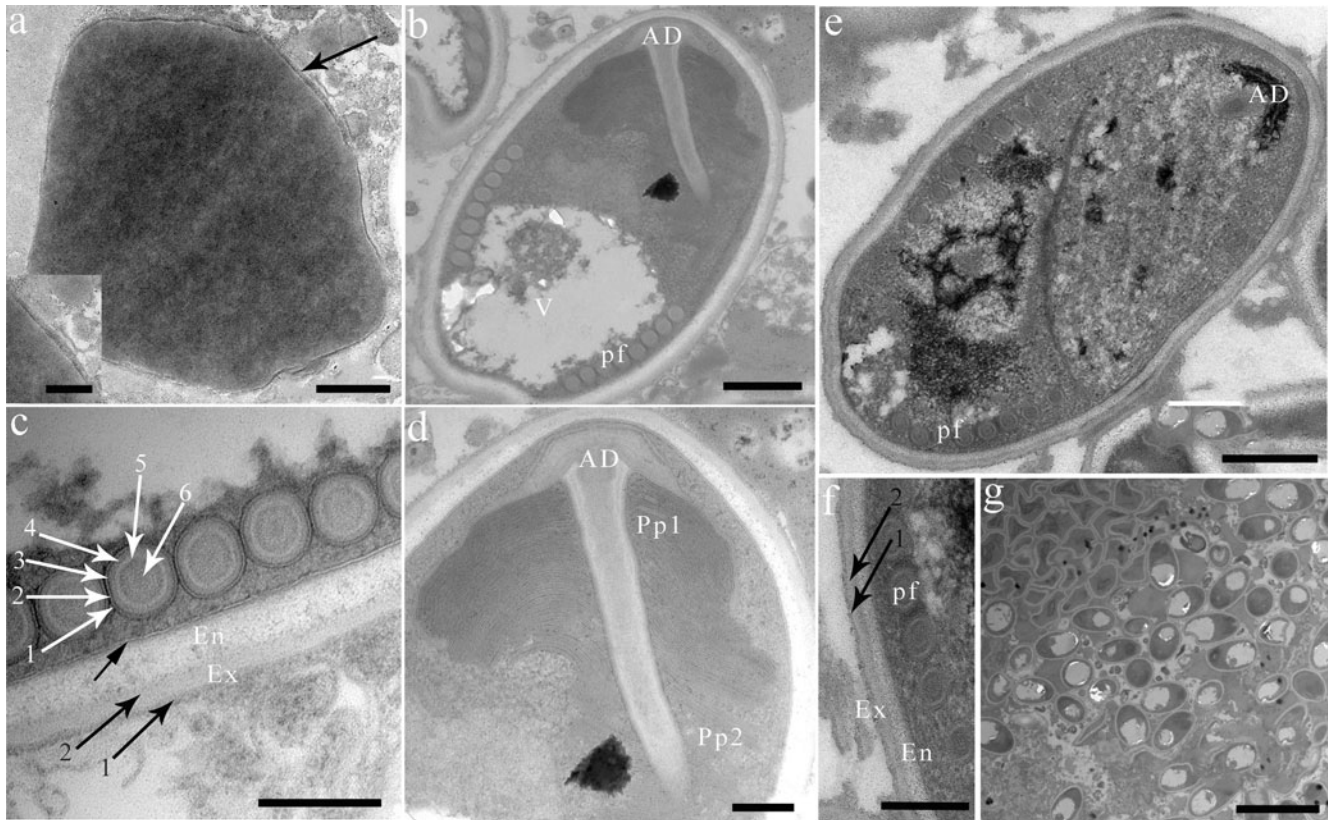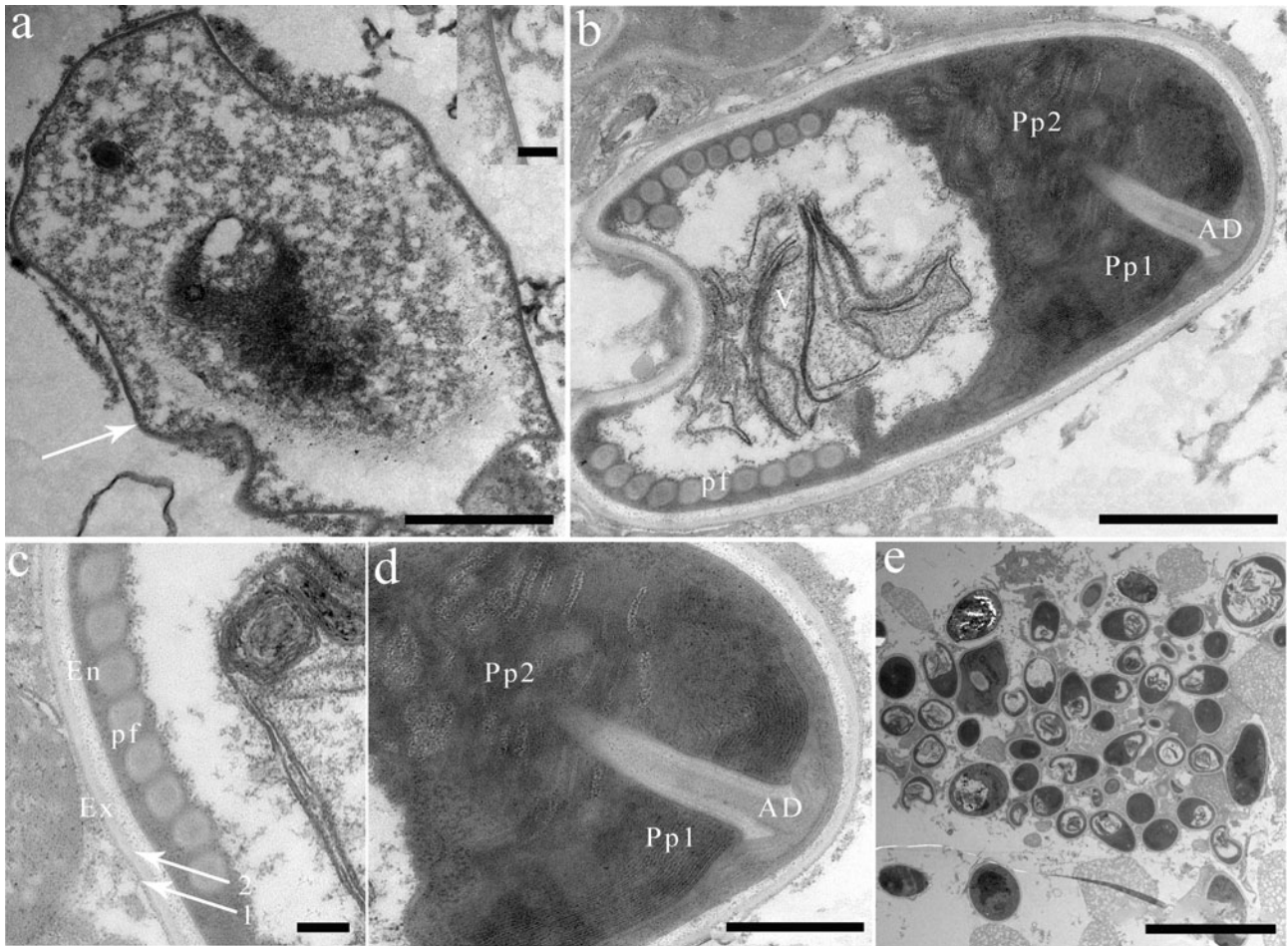
Fig. 3. Electron microscopy of *Ovipleistophora diplostomuri*. (a) Irregular sporoblasts of *O. diplostomuri* isolated from *Culter alburnus* surrounding by a thick electron-dense membrane (arrow). Magnification of the thick electron-dense membrane (inset in a). Scale bar = 500 nm. (b) A mature spore of *O. diplostomuri* isolated from *Culter alburnus* with typical microsporidian features of internal structure, including the isofilar polar filaments (pf), a bipartite polaroplast, a vacuole (V), a mushroom-shaped anchoring disc (AD) and a trilaminar spore wall consisting of an electron-dense exospore, an electron-translucent endospore and a plasma membrane. Scale bar = 500 nm. (c) Magnification of the exospores (Ex) showing two distinct layers (layer 1 and layer 2). Trilaminar spores wall consisting of exospore (Ex), endospore (En) and plasma membrane (short black arrow). Transverse section of polar filament coils exhibiting six discontinuous density concentric circles. Scale bar = 200 nm. (d) Bipartite polaroplast consisting narrow lamellae (Pp1) and wide lamellae (Pp2). Scale bar = 200 nm. (e) A mature spore of *O. diplostomuri* isolated from *Xenocypris argentea* with eight coils of polar filament (pf) and anchoring disc (AD). Scale bar = 500 nm. (f) Magnification of the exospores (Ex) showing two distinct layers (layer 1 and layer 2). Scale bar = 200 nm. (g) Mature spores occur in direct contact with the host cell cytoplasm. Scale bar = 5 μm.

Molecular characterization

Three SSU sequences of the microsporidian species from *C. alburnus*, *X. argentea* and *P. pekinensis* were successfully amplified and the obtained consensus sequences were individually deposited in GenBank under accession numbers MW811110, MW811108 and MW811109, respectively. As such, their concatenated partial SSU, complete ITS and partial LSU was respectively assigned with accession numbers MW811107, MW811105 and MW811106. Blast searches and sequence comparison analysis showed the closest identity of these sequences with several *Ovipleistophora* species. SSU rDNA sequence obtained from *C. alburnus* and *X. argentea* is 99.68% identical, which is the highest identical to that of *O. diplostomuri* (MN515056 with 99.79% and 99.57% identity, respectively). Their next closest identities were to *O. diplostomuri* (KY809102 with 99.36% and 99.37% identity, respectively) and *O. arlo* (MH911630 with 98.93% and 99.04% identity, respectively). However, the SSU rDNA sequence obtained from *P. pekinensis* is most identical to *O. ovariae* (99.58% identity) and only 98.18% and 98.61% identical with that from *C. alburnus* and *X. argentea*, respectively. The pairwise distances/ similarities calculated by Kimura 2-parameter model between SSU rDNA sequences of *Ovipleistophora* species and 2 other microsporidian species of high sequence similarity ranged from 0.002/99.79% (between the species from *C. alburnus* MW811110 and *O. diplostomuri* MN515056) to 0.055/94.54% (between *O. ovariae* AJ252850 and *Heterosporis anguillarum* AF387331) (Table 2). Therefore, from the morphological and

high SSU rDNA sequence identity, the species from *C. alburnus* and *X. argentea* can be determined to be conspecific to *O. diplostomuri* and species from *P. pekinensis* to be *O. ovariae*. To further explore the possible genetic variation among isolates of *O. diplostomuri* from different hosts, their full ITS and partial LSU rDNA sequences comparison analysis were performed. Results clearly indicated that the between-host genetic variation of the ITS sequences was distinct. ITS rDNA sequence of the isolates from *C. alburnus* and *X. argentea* was 97.9% similar, but only 85.7% and 87.8% similar to that of the isolate (KY809102) from the bluegill sunfish *L. marcrochirus* and its digenean parasite, *P. minimum* (Table 3). As such, between-host variations among the partial LSU rDNA sequences of three *O. diplostomuri* hosts were distinctly higher that those among their SSU rDNA sequences. LSU sequences of the isolates from *C. alburnus* and *X. argentea* were 99.0% identical, but only 96.2% identical with that from the typical host of *O. diplostomuri* (Table 3). Nineteen single polymorphism sites (SNPs) was found among the partial LSU rDNA gene sequences (about 440 bp) of three isolates of *O. diplostomuri* (KY809102) (Table 4). Bayesian and maximum likelihood analyses of the aligned SSU rDNA gene sequences of 22 microsporidian species generated highly similar topologies, although with different support values at some branch nodes. The results showed that the genus *Ovipleistophora* was monophyletic which grouped with *Pleistophora* and *Heterosporis* into an independent clade. The *O. diplostomuri* isolates infecting the ovary of *C. alburnus* and *X. argentea* clustered with the isolate

Fig. 4. Electron microscopy of *Ovipleistophora ovariae*. (a) Irregular sporoblasts of *O. ovariae* isolated from *Parabramis pekinensis* surrounding by three-layered electron-dense membrane (arrow). Magnification of the three-layered electron-dense membrane (inset in a). Scale bar = 1 μm. (b) A mature microspore of *O. ovariae* with typical microsporidian features of internal structure, including isofilar polar filaments (pf), bipartite polaroplast (Pp1, Pp2), vacuole (V) and mushroom-shaped anchoring (AD). Scale bar = 1 μm. (c) Trilaminar spores wall including an electron-dense exospore, an electron-translucent endospore and a plasma membrane. Exospore showing two distinct layers (layer 1 and layer 2). Scale bar = 200 nm. (d) Bipartite polaroplast (Pp1, Pp2) and mushroom-shaped anchoring disc (AD). Scale bar = 500 nm. (e) Mature spores occur in direct contact with the host cell cytoplasm. Scale bar = 10 μm.

infecting the musculature of *P. bivittatus* collected from the USA to form an independent branch, but excluding the *L. marcrochirus* isolate collected from the USA. The *O. ovariae* isolate from the ovary of *P. pekinensis* clustered with the isolate from the ovary of *Notemigonus crysoleucas* with a high support value (Fig. 6).

Discussion

To discriminate freshwater fish oocyte-infecting species originally assigned to the genus *Pleistophora* from other congeneric species, Pekkarinen *et al.* (2002) erected the genus *Ovipleistophora*. Four species, *O. mirandellae*, *O. ovariae*, *O. diplostomuri* and *O. arlo* have been so far formally described with morphological, ultrastructural and molecular features. Based on the definitive features of the genus *Ovipleistophora* and the high SSU rDNA sequence identity, the pathogen from *C. alburnus* and *X. argentea* can be identified to be *O. diplostomuri* and the parasite from *P. pekinensis* to be *O. ovariae*, although there are not all morphologically consistent with those of the previously reported isolates (Table 5). This is the first report of fish-infecting *Ovipleistophora* in Asia. In the present work, only monomorphic microspores of *O. diplostomuri* were found. However, dimorphic spores were firstly reported herein for *O. ovariae*. Dimorphic spores (macrospores and microspores) have been reported in several fish-infecting microsporidian genera, such as *Pleistophora* and *Heterosporis* (Al-Quraishy *et al.*, 2012; Kent *et al.*, 2014; El-Garhy *et al.*, 2017), which was also thought

to be the definitive taxonomic feature of *Ovipleistophora* (Maurand *et al.*, 1988; Pekkarinen *et al.*, 2002). At present, the mechanisms underlying the occurrence of two types of spores for some species and the respective functionality of microspores and macrospores remain unknown. Furthermore, the development of *O. diplostomuri* and *O. ovariae* herein were found to be in direct contact with the host cell cytoplasm, rather than within sporophorous vesicles which was one of the definitive taxonomic features of the genus *Ovipleistophora* and was present in the previously reported isolates of *O. diplostomuri* and *O. ovariae* (Kent *et al.*, 2014; Lovy and Friend, 2017). The absence of sporophorous vesicles was also previously reported for the development of *O. ovariae* infecting the fathead minnows, *Pimephales promelas* (Ruehl-Fehlert *et al.*, 2005). So, the developmental pattern referred from the ultrastructural observations was suggested not to be the reliable taxonomic criterion of the genus *Ovipleistophora* for the plasticity derived from the habitat adaptation, including host, infection sites and host habitat environment.

In terms of host, *Ovipleistophora* species were originally restricted to freshwater fish (Pekkarinen *et al.*, 2002). With the subsequent increasing diversity, the genus *Ovipleistophora* was supposed to have a broad host range or a complex lifecycle between fish and crustacean (Stentiford *et al.*, 2018; Bojko *et al.*, 2020). Additionally, the cyst wall of the digenean parasite *P. minimum* of the bluegill sunfish was also found to be simultaneously infected by *O. diplostomuri* which further extended the host range
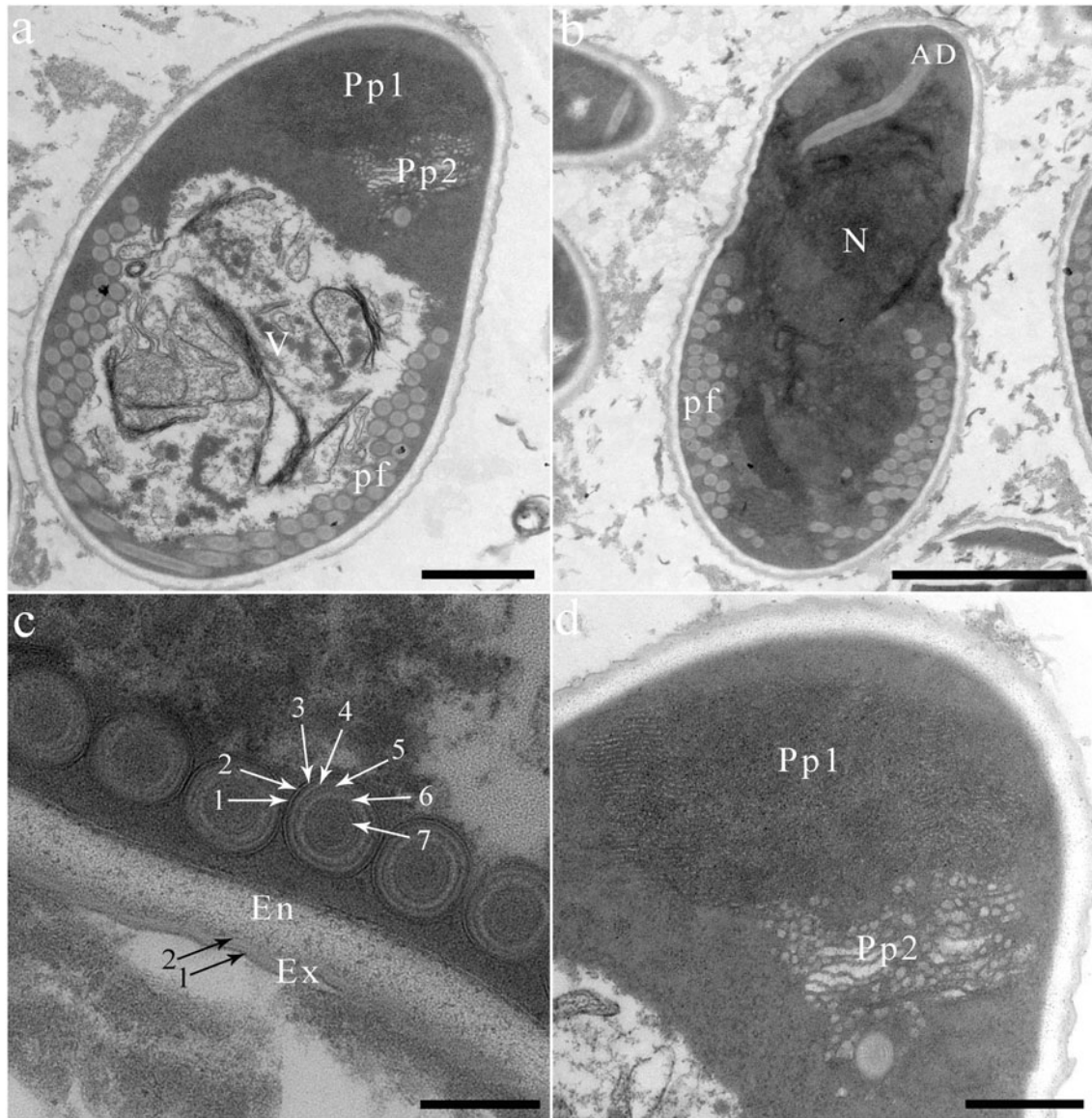
Fig. 5. Electron microscopy of *Ovipleistophora ovariae*. (a) A mature macrospores of *O. ovariae* shows bipartite polaroplast (Pp1, Pp2), a vacuole (V) and isofilar polar filaments. Scale bar = 1 μm. (b) A mature macrospore of *O. ovariae* contains a mushroom-shaped anchoring disc (AD), a large nucleus (N) and isofilar polar filament (pf). Scale bar = 2 μm. (c) Transverse section of polar filament coils exhibiting seven discontinuous density concentric circles. Trilaminar spores wall consisting of an electron-dense exospore, an electron-translucent endospore and a plasma membrane. Exospore showing an electron-dense layer (layer 1) and a moderately electron-dense layer (layer 2). Scale bar = 200 nm. (d) Bipartite polaroplast with anterior lamellae (Pp1) and posterior tubules (Pp2). Scale bar = 500 nm.

of *Ovipleistophora* species. A wide host range has been previously reported for other microsporidian taxa including the genus *Amblyospora* (Andreadis *et al.*, 2018), *Paranucleospora theridion* (Nylund *et al.*, 2010), *Hyalinocysta chapmani* (Andreadis and Vossbrinck, 2002) and *Parathelohania anophelis* (Avery and Undeen, 1990). Wide host range is one of the factors to derive the polymorphic development and the occurrence of between-host morphologically and functionally distinct spores for an individual microsporidian species. Interestingly, the developmental features of *Ovipleistophora* species were inconsistent with those of taxa with a wide host range which were generally characterized by the presence of diplokaryotic meronts and polysporoblastic sporogony and haploid meiospores. However, the presence of the isolated nuclei during the whole life cycle and a single sporulation sequence were the typical features of *O. mirandellae*, *O. diplostomuri* and *O. ovariae*. This can partially explain why *Ovipleistophora* possesses dimorphic spores with similar structures. Screening the possible crustacean host of *O. diplostomuri* and *O. ovariae* in the sympatric wetlands of this sampling will facilitate to extend their host range.

Originally, the genus *Ovipleistophora* was defined to be the obligate parasite of the fish ovary (Pekkarinen *et al.*, 2002). However, Lovy and Friend (2017) found that *O. diplostomuri* infected both the liver of bluegill sunfish *L. macrochirus* and the cyst wall of the digenean parasite *P. minimum*. Furthermore, *O. diplostomuri* and *O. arlo* was subsequently recorded in muscle tissue of the freshwater crayfish and the common pawn, respectively (Stentiford *et al.*, 2018; Bojko *et al.*, 2020). So, it can be supposed that the infection sites of *Ovipleistophora* species from vertebrate and invertebrate hosts are diverse with the high diversity being uncovered in future, although fish ovary is still the common infection site.

Ribosomal DNA genes have been widely applied into the species identification, classification and intraspecific discrimination of Microsporidia for it cover not only comparative loci but also highly variable loci (Haro *et al.*, 2003; Santín and Fayer, 2009; Krebes *et al.*, 2010; Malcekova *et al.*, 2011; Li *et al.*, 2012a; Pombert *et al.*, 2013; González-Tortuero *et al.*, 2016; Xu *et al.*, 2020). In the present study, we proved for the first time the

Table 2. Pairwise nucleotide sequence identity (upper right) values and evolutionary distances (left bottom) among *Ovipleistophora* species/isolates and two other microsporidian species with high sequence similarity by Kimura-2 Parameter analysis based on SSU rDNA sequences

Species (GenBank accession number)	1	2	3	4	5	6	7	8	9	10	11
1. *Ovipleistophora diplostomuri* MW811110	–	99.68	98.18	99.79	99.36	98.93	98.61	98.28	97.96	96.74	95.11
2. *O. diplostomuri* MW811108	0.0032	–	98.61	99.57	99.37	99.04	98.72	98.39	98.40	96.85	95.22
3. *Ovipleistophora ovariae* MW811109	0.0182	0.0139	–	98.07	98.61	97.85	97.75	97.09	99.58	96.08	94.77
4. *O. diplostomuri* MN515056	0.0021	0.0043	0.0193	–	99.36	99.04	98.72	98.50	97.86	96.86	95.23
5. *O. diplostomuri* KY809102	0.0064	0.0064	0.0139	0.0064	–	98.83	98.72	98.07	98.40	96.75	95.11
6. *Ovipleistophora arlo* MH911630	0.0107	0.0096	0.0215	0.0096	0.0117	–	99.47	98.93	97.64	96.41	95.12
7. *Ovipleistophora mirandellae* AF356223	0.0139	0.0128	0.0225	0.0128	0.0128	0.0053	–	98.72	97.53	96.07	94.77
8. *O. mirandellae* AJ252954	0.0172	0.0161	0.0291	0.0150	0.0193	0.0107	0.0128	–	96.87	95.96	94.66
9. *O. ovariae* AJ252850	0.0204	0.0160	0.0042	0.0214	0.0160	0.0236	0.0247	0.0313	–	95.86	94.54
10. *Pleistophora hyphessobryconis* KM458272	0.0326	0.0315	0.0392	0.0314	0.0325	0.0359	0.0393	0.0404	0.0414	–	95.68
11. *Heterosporis anguillarum* AF387331	0.0489	0.0478	0.0523	0.0477	0.0489	0.0488	0.0523	0.0534	0.0546	0.0432	–

Table 3. Percentage of sequence similarity of the *Ovipleistophora diplostomuri* isolated from different hosts

Hosts	Gene		
	SSU	ITS	LSU
Culter alburnus vs *Lepomis macrochirus*	99.3	85.7	96.2
Xenocypris argentea vs *L. macrochirus*	99.2	87.8	96.2
C. alburnus vs *X. argentea*	99.7	97.9	99.0

between-host variation of ITS and LSU sequences of *O. diplosto-muri* and the conservative SSU rDNA sequences of all three *O. diplostomuri* isolates. The intraspecific conservative SSU rDNA sequence of *O. diplostomuri* is similar with most of the fish-infecting microsporidian taxa, rather than insect-infecting microsporidia, such as *Nosema ceranae* (Sagastume *et al.*, 2011) and *Dictyocoela* spp. (Krebes *et al.*, 2010; Wilkinson *et al.*, 2011). These results indicate that SSU rDNA sequence can be used as a suitable molecular marker for the identification of *O. diplostomuri* and ITS and LSU rDNA sequence are a good molecular marker to discriminate the intraspecific isolates of this pathogen.

Intraspecific genetic variations are common among Microsporidia, especially for insect-infecting species, such as *Nosema ceranae* (Sagastume *et al.*, 2011), *N. bombi* (Cordes *et al.*, 2012), *N. apis* (Maside *et al.*, 2015), *N. granulosis* (Ironside, 2013) and *N. bombycis* (Ironside, 2013; Liu *et al.*, 2013). However, the mechanisms to cause the intra-isolate copy variation of SSU rDNA sequence and the inter-isolate variation of ITS or LUS rDNA sequence remain unclear. Host shift was thought to be one of the possible factors to derive species differentiation. Chaimanee *et al.* (2011) found that *N. ceranae* isolated from different host species formed different branches. Maside *et al.* (2015) found that the genetic variation of the *N. apis* occurred among isolates from the honey bee of different lineages. Few studies concern the possible phenotypic changes of isolates with genetic variation referred from the difference of ITS and LUS sequences. Between-host ultrastructural differences of *Pleistophora hyphessobryconis* were documented (Li *et al.*, 2012*b*). Phylogenetic analysis indicated that *O. diplostomuri* isolated from the liver of bluegill sunfish *L. macrochirus* (Perciformes) and the digenean parasite *P. minimum* in North America was an independent branch, rather than clustering with *O. diplostomuri* isolated from *C. alburnus* (Cypriniformes) and *X. argentea* (Cypriniformes) in China, indicating that host affinity and geographical distribution provide the possible evolutionary signal for the species differentiation in some extents. As such, *O. mirandellae* isolated from the ovary of *Gymnocephalus cernuus* (Perciformes) clustered with *O. arlo*, rather than clustering with *O. mirandellae* isolated from Cypriniformes to form an independent branch. According to our speculation, the potential fish host of *O. arlo* possibly belongs to Cypriniformes.

Genetic variation of a parasite can cause different disease consequences (Branchiccela *et al.*, 2017; Shaw *et al.*, 2021; Taggart-Murphy *et al.*, 2021). No inflammatory responses occurred in the ovary of *C. alburnus*, *X. argentea* and *P. pekinensis* for fish ovary is a general immune-privileged site. Given the possible more variable infection sites of *O. diplostomuri* and *O. ovariae*, ITS or LUS rDNA will be a feasible molecular marker for determining the virulent and avirulent isolates.

In summary, this present study reports for the first time two *Ovipleistophora* species infecting the ovary of three cyprinid fish in China which extends their host range and host geographical

Table 4. The partial LSU rDNA gene sequences (440 bp) of *Ovipleistophora diplostomuri* isolated from different hosts show the single nucleotide polymorphism sites (SNPs)

Host	SNPs																		
	91	96	107	189	190	211	219	222	239	240	242	244	250	251	304	305	307	369	438
Lepomis macrochirus KY809102	A	T	A	A	G	C	G	A	G	T	T	A	A	C	T	C	A	A	–
Culter alburnus MW811107	T	–	G	G	C	T	A	A	A	G	–	G	G	T	A	G	T	A	T
Xenocypris argentea MW811105	T	–	G	G	C	T	A	G	A	A	–	G	G	T	T	G	A	G	T
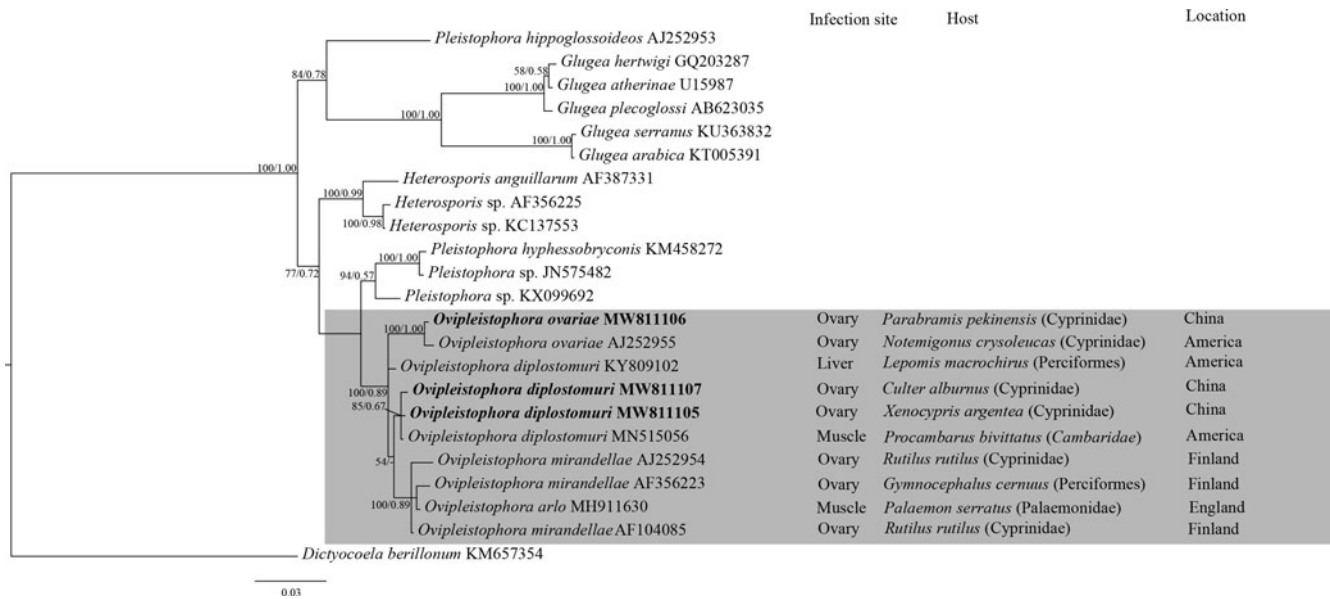
Fig. 6. The SSU rDNA-inferred phylogenetic relationships between *Ovipleistophora* species and the other aligned microsporidian species by Bayesian Inference (BI) method. The species names are followed by GenBank accession number. BI posterior probabilities were shown firstly, followed by ML support values on branch nodes. The present species was highlighted in bold. The infection site and host, as well as the geographical location of species belonging to *Ovipleistophora* spp. were presented.

Table 5. Morphological comparison of *Ovipleistophora* spp.

Species	Host	Infected site	Spores size (μm)	Polar filament	Polaroplast	Exospore	Parasite-host interface	References
O. diplostomuri	*Culter alburnus*	Ovary	Only one type of spore 4.03 × 2.63	8–10 coils in one row	Closely packed anterior and wider posterior lamellae	Two-layered	Direct contact with host cell cytoplasm	(herein)
O. diplostomuri	*Xenocypris argentea*	Ovary	Only one type of spore 4.03 × 1.96	8–10 coils in one row	(–)	Two–layered	Direct contact with host cell cytoplasm	(herein)
O. ovariae	*Parabramis pekinensis*	Ovary	Macrospores 9.26 × 4.90 Microspores 4.17 × 2.72	19–34 coils in 2–3 rows 6–10 coils in one row	Lamellar anterior and tubular posterior parts	Two-layered	Direct contact with host cell cytoplasm	(herein)
O. diplostomuri	*Lepomis macrochirus Posthodiplostomum minimum*	Liver, spleen, kidney, epicardium Metacercarial cyst wall	Microspores 4.3 × 2.5 Macrospores 7.5 × 4.7	6–9 coils in one row 19–43 coils in four rows	Closely packed anterior and wider posterior lamellae	(–)	Sporophorous vesicle with 22 microspores and 6 macrospores	Lovy and Friend (2017)

(*Continued*)

Table 5. (*Continued.*)

Species	Host	Infected site	Spores size (μm)	Polar filamant	Polaroplast	Exosphere	Parasite-host interface	References
O. diplostomuri	*Procambarus bivittatus*	Musculature	(–)	(–)	(–)	(–)	Sporophorous vesicle with more than 16 spores	Bojko *et al.* (2020)
O. arlo	*Palaemon serratus*	Skeletal musculature	Only one type of spore 4.24 × 2.26	Eight coils in one row	Closely packed anterior and wider posterior lamellae	Four-layered	Sporophorous vesicle with more than 16 spores	Stentiford *et al.* (2018)
O. ovariae	*Notemigonus crysoleucas*	Ovary	Only one type of spore 8.42 × 4.24	(–)	(–)	(–)	Sporophorous vesicle with more than 14 spores	Maurand *et al.* (1988), Ruehl-Fehlert *et al.* (2005)
O. mirandellae	*Alburnus mirandellae*	Ovary, testis	Microspores 8–9 × 4 Macrospores 3.50 × 2	10 coils in row 40 coils in four rows	Wider anterior and closely packed posterior lamellae	(–)	Sporophorous vesicle with 8–125 microspores and 32 macrospores	Maurand *et al.* (1988)

distribution. Distinct genetic variations were found in the between-host *O. diplostomuri* isolates.

References

Al-Quraishy S, Abdel-Baki AS, Al-Qahtani H, Dkhil M, Casal G and Azevedo C (2012) A new microsporidian parasite, *Heterosporis saurida* n. sp. (Microsporidia) infecting the lizardfish, *Saurida undosquamis* from the Arabian Gulf, Saudi Arabia: ultrastructure and phylogeny. *Parasitology* **139**, 454–462.

Andreadis TG and Vossbrinck CF (2002) Life cycle, ultrastructure and molecular phylogeny of *Hyalinocysta chapmani* (Microsporidia: Thelohaniidae), a parasite of *Culiseta melanura* (Diptera: Culicidae) and *Orthocyclops modestus* (Copepoda: Cyclopidae). *Journal of Eukaryotic Microbiology* **49**, 350–364.

Andreadis TG, Thomas MC and Shepard JJ (2018) *Amblyospora khaliulini* (Microsporidia: Amblyosporidae): investigations on its life cycle and ecology in *Aedes communis* (Diptera: Culicidae) and *Acanthocyclops vernalis* (Copepoda: Cyclopidae) with redescription of the species. *Journal of Invertebrate Pathology* **151**, 113–125.

Avery SW and Undeen AH (1990) Horizontal transmission of *Parathelohania anopheles* to the copepod, *Microcyclops varicans*, and the mosquito, *Anopheles quadrimaculatus. Journal of Invertebrate Pathology* **56**, 98–105.

Baker MD, Vossbrinck CR, Didier ES, Maddox JV and Shadduck JA (1995) Small subunit ribosomal DNA phylogeny of various microsporidia with emphasis on AIDS-related forms. *Journal of Eukaryotic Microbiology* **42**, 564–570.

Bojko J, Behringer DC, Moler P and Reisinger L (2020) *Ovipleistophora diplostomuri*, a parasite of fish and their trematodes, also infects the crayfish *Procambarus bivittatus. Journal of Invertebrate Pathology* **169**, 107306.

Branchiccela B, Arredondo D, Higes M, Invernizzi C, Martín-Hernández R, Tomasco I, Zunino P and Antúnez K (2017) Characterization of *Nosema ceranae* genetic variants from different geographic origins. *Microbial Ecology* **73**, 978–987.

Cali A and Takvorian PM (2014) Developmental morphology and life cycles of the Microsporidia. In Weiss LM and Becnel JJ (eds), *Microsporidia: Pathogens of Opportunity*. Oxford: Wiley Blackwell, pp. 71–133.

Chaimanee V, Chen YP, Pettis JS, Cornman RS and Chantawannakul P (2011) Phylogenetic analysis of *Nosema ceranae* isolated from European and Asian honeybees in Northern Thailand. *Journal of Invertebrate Pathology* **107**, 229–233.

Cordes N, Huang WF, Strange JP, Cameron SA, Griswold TL, Lozier JD and Solter LF (2012) Interspecific geographic distribution and variation of the pathogens *Nosema bombi* and *Crithidia* species in United States bumble bee populations. *Journal of Invertebrate Pathology* **109**, 209–216.

El-Garhy M, Cali A, Morsy K, Bashtar AR and Al-Quraishy S (2017) Ultrastructural characterization of *Pleistophora macrozoarcidis* Nigerelli 1946 (Microsporidia) infecting the ocean pout *Macrozoarces americanus* (Perciformes, Zoarcidae) from the Gulf of Maine, MA, USA. *Parasitology Research* **116**, 61–71.

Gatehouse HS and Malone LA (1998) The ribosomal RNA gene region of *Nosema apis* (Microspora): DNA sequence for small and large subunit rRNA genes and evidence of a large tandem repeat unit size. *Journal of Invertebrate Pathology* **71**, 97–105.

González-Tortuero E, Rusek J, Maayan I, Petrusek A, Piálek L, Laurent S and Wolinska J (2016) Genetic diversity of two daphnia-infecting microsporidian parasites, based on sequence variation in the internal transcribed spacer region. *Parasites Vectors* **9**, 293.

Hall TA (1999) BioEdit: a user-friendly biological sequence alignment editor and analysis program for Windows 95/98/NT. *Nucleic Acids Symposium Series* **41**, 95–98.

Haro M, del Águila C, Fenoy S and Henriques-Gil N (2003) Intraspecies genotype variability of the microsporidian parasite *Encephalitozoon hellem. Journal of Clinical Microbiology* **41**, 4166–4171.

Ironside JE (2013) Diversity and recombination of dispersed ribosomal DNA and protein-coding genes in microsporidia. *PLoS One* **8**, e55878.

Kent ML, Shaw RW and Sanders JL (2014) Microsporidia in fish. In Weiss LM and Becnel JJ (eds), *Microsporidia: Pathogens of Opportunity*. Oxford: Wiley Blackwell, pp. 493–520.

Krebes K, Blank M, Frankowski J and Bastrop R (2010) Molecular characterisation of the Microsporidia of the amphipod *Gammarus duebeni* across its natural range revealed hidden diversity, wide-ranging prevalence and potential for co-evolution. *Infection Genetics and Evolution* **10**, 1027–1038.

Li JL, Chen WF, Wu J, Peng WJ, An JD, Schmid-Hempel P and Schmid-Hempel R (2012*a*) Diversity of *Nosema* associated with bumblebees (*Bombus* spp.) from China. *International Journal for Parasitology* **42**, 49–61.

Li KB, Chang OQ, Wang F, Liu C, Liang HL and Wu SQ (2012*b*) Ultrastructure, development, and molecular phylogeny of *Pleistophora hyphessobryconis*, a broad host microsporidian parasite of *Puntius tetrazona*. *Parasitology Research* **111**, 1715–1724.

Liu HD, Pan GQ, Luo B, Li T, Yang Q, Vossbrinck CR, Debrunner-Vossbrinck BA and Zhou ZY (2013) Intraspecific polymorphism of rDNA among five *Nosema bombycis* isolates from different geographic regions in China. *Journal of Invertebrate Pathology* **113**, 63–69.

Liu XH, Xu LW, Luo D, Zhao YL, Zhang QQ, Liu GF and Zhang JY (2018) Outbreak of mass mortality of yearling groupers of *Epinephelus* (Perciformes, Serranidae) associated with the infection of a suspected new enteric *Sphaerospora* (Myxozoa: Myxosporea) species in South China Sea. *Journal of Fish Diseases* **41**, 663–672.

Liu XH, Stentiford GD, Voronin VN, Sato H, Li AH and Zhang JY (2019) *Pseudokabatana alburnus* n. gen. n. sp., (Microsporidia) from the liver of topmouth culter *Culter alburnus* (Actinopterygii, Cyprinidae) from China. *Parasitology Research* **118**, 1689–1699.

Lovy J and Friend SE (2017) Phylogeny and morphology of *Ovipleistophora diplostomuri* n. sp. (Microsporidia) with a unique dual-host tropism for bluegill sunfish and the digenean parasite *Posthodiplostomum minimum* (Strigeatida). *Parasitology* **144**, 1898–1911.

Malcekova B, Valencakova A, Luptakova L, Molnar L, Ravaszova P and Novotny F (2011) First detection and genotyping of *Encephalitozoon cuniculi* in a new host species, gyrfalcon (*Falco rusticolus*). *Parasitology Research* **108**, 1479–1482.

Maside X, Gómez-Moracho T, Jara J, Martín-Hernández R, Rúa PD, Higes M and Bartolomé C (2015) Population genetics of *Nosema apis* and *Nosema ceranae*: one host (*Apis mellifera*) and two different histories. *PLoS One* **10**, e0145609.

Maurand J, Loubes C, Gasc C, Pelletier J and Barral J (1988) *Pleistophora mirandellae* Vaney & Conte, 1901, a microsporidian parasite in cyprinid fish of rivers in Hérault: taxonomy and histopathology. *Journal of Fish Diseases* **11**, 251–258.

Nylund S, Nylund A, Watanabe K, Arnesen CE and Karlsbakk E (2010) *Paranucleospora theridion* n. gen., n. sp. (Microsporidia, Enterocytozoonidae) with a life cycle in the salmon louse (*Lepeophtheirus salmonis*, Copepoda) and Atlantic salmon (*Salmo salar*). *Journal of Eukaryotic Microbiology* **57**, 95–114.

Park E and Poulin R (2021) Revisiting the phylogeny of microsporidia. *International Journal for Parasitology* **51**, 855–864.

Pekkarinen M, Lom J and Nilsen F (2002) *Ovipleistophora* gen. n., a new genus for *Pleistophora mirandellae*-like microsporidia. *Diseases of Aquatic Organisms* **48**, 133–142.

Pombert JF, Xu J, Smith DR, Heiman D, Young S, Cuomo CA, Weiss LM and Keeling PJ (2013) Complete genome sequences from three genetically distinct strains reveal high intraspecies genetic diversity in the microsporidian *Encephalitozoon cuniculi*. *Eukaryotic Cell* **12**, 503–511.

Ruehl-Fehlert C, Bomke C, Dorgerloh M, Palazzi X and Rosenbruch M (2005) *Pleistophora* infestation in fathead minnows, *Pimephales promelas* (Rafinesque). *Journal of Fish Diseases* **28**, 629–637.

Sagastume S, del Aguila C, Martín-Hernández R, Higes M and Henriques-Gil N (2011) Polymorphism and recombination for rDNA in the putatively asexual microsporidian *Nosema ceranae*, a pathogen of honeybees. *Environmental Microbiology* **13**, 84–95.

Santín M and Fayer R (2009) *Enterocytozoon bieneusi* genotype nomenclature based on the internal transcribed spacer sequence: a consensus. *Journal of Eukaryotic Microbiology* **56**, 34–38.

Shaw CL, Bilich R, O'Brien B, Cáceres CE, Hall SR, James TM and Duffy MA (2021) Genotypic variation in an ecologically important parasite is associated with host species, lake and spore size. *Parasitology* **148**, 1303–1312.

Smith JE (2009) The ecology and evolution of microsporidian parasites. *Parasitology* **136**, 1901–1914.

Stentiford GD, Bateman KS, Feist SW, Stone DM and Dunn AM (2013) Microsporidia: diverse, dynamic and emergent pathogens in aquatic systems. *Trends in Parasitology* **29**, 567–578.

Stentiford GD, Ross S, Minardi D, Feist SW, Bateman KS, Gainey PA and Bass D (2018) Evidence for trophic transfer of *Inodosporus octospora* and *Ovipleistophora arlo* n. sp. (Microsporidia) between crustacean and fish hosts. *Parasitology* **145**, 1105–1117.

Summerfelt RC and Goodwin AE (2010) Ovipleistophoriasis: a microsporidian disease of the golden shiner ovary. In *American Fisheries Society-Fish Health Section Blue Book: Suggested Procedures for the Detection and Identification of Certain Finfish and Shellfish Pathogens*, 1.3.2.3, 2016 Edn. Accessible at: http://afs-fhs.org/bluebook/bluebook-index.php.

Taggart-Murphy L, Alama-Bermejo G, Dolan B, Takizawa F and Bartholomew J (2021) Differences in inflammatory responses of rainbow trout infected by two genotypes of the myxozoan parasite *Ceratonova shasta*. *Developmental and Comparative Immunology* **114**, 103829.

Tamura K, Stecher G, Peterson D, Filipski A and Kumar S (2013) MEGA6: molecular evolutionary genetics analysis version 6.0. *Molecular Biology Evolution* **30**, 2725–2729.

Thompson JD, Gibson TJ, Plewniak F, Jeanmougin F and Higgins DG (1997) The CLUSTAL X Windows interface: flexible strategies for multiple sequence alignment aided by quality analysis tools. *Nucleic Acids Research* **25**, 4876–4883.

Tsai SJ, Kou GH, Lo CF and Wang CH (2002) Complete sequence and structure of ribosomal RNA gene of *Heterosporis anguillarum*. *Diseases of Aquatic Organisms* **49**, 199–206.

Vávra J and Lukeš J (2013) Microsporidia and 'the art of living together'. *Advances in Parasitology* **82**, 253–319.

Vávra J, Hyliš M, Fiala I, Sacherová V and Vossbrinck CR (2017) Microsporidian genus *Berwaldia* (Opisthosporidia, Microsporidia), infecting daphnids (Crustacea, Branchiopoda): biology, structure, molecular phylogeny and description of two new species. *European Journal of Protistology* **61**, 1–12.

Weiss LM and Vossbrinck CR (1999) Molecular biology, molecular phylogeny, and molecular diagnostic approaches to the microsporidia. In Wittner M and Weiss LM (eds), *The Microsporidia and Microsporidiosis*. Washington: ASM Press, pp. 129–171.

Wilkinson TJ, Rock J, Whiteley NM, Ovcharenko MO and Ironside JE (2011) Genetic diversity of the feminising microsporidian parasite *Dictyocoela*: new insights into host-specificity, sex and phylogeography. *International Journal for Parasitology* **41**, 959–966.

Xu J, Wang X, Jing HQ, Cao SK, Zhang XF, Jiang YY, Yin JH, Cao JP and Shen YJ (2020) Identification and genotyping of *Enterocytozoon bieneusi* in wild Himalayan marmots (*Marmota himalayana*) and Alashan ground squirrels (*Spermophilus alashanicus*) in the Qinghai-Tibetan Plateau area (QTPA) of Gansu Province, China. *Parasites Vectors* **13**, 367.